POAC'17
Busan, KOREA

Proceedings of the 24th International Conference on
Port and Ocean Engineering under Arctic Conditions
June 11-16, 2017, Busan, Korea

Bi-Polar Full-Scale Measurements of Operational Loading on Polar Vessel Shaft-Lines

Rosca J.O. de Waal[1], Anriëtte Bekker[1], P. Stephan Heyns[2]

[1] Sound and Vibration Research Group, Stellenbosch University, Stellenbosch, South Africa

[2] Centre for Asset Integrity Management , University of Pretoria, Pretoria, South Africa

ABSTRACT

The port side shaft-lines of two polar research vessels, the SA Agulhas II and the FS Polarstern, were instrumented with in-board strain gauges to capture operational measurements of shear strain and axial strain. These measurements were used to calculate the instantaneous torque and thrust in the respective shafts. Vessel operations were categorized into open water navigation, ice passage and stationary operations. Subsequent to this rainflow counting of the transient torque and thrust cycles was performed in order to gain insight into the respective demands of different operational environments. During the 2015/2016 Antarctic relief voyage of the SA Agulhas II the vessel spent 16% of its voyage duration in ice and a further 54% in open water navigation. In comparison the FS Polarstern was engaged in ice passage for 24% of its Arctic voyage from Tromsø and spent the majority of her time performing stationary operations. Although both vessels experienced similar levels of torsional loading, the SA Agulhas II shaft line was more critically loaded relative to its Maximum Continuous Rating.

KEY WORDS: Shaft loads; Rainflow counting; Torque; Thrust; Ice.

INTRODUCTION

Efficient and safe shipping in Arctic regions is an increasing requirement as maritime transport in ice-covered seas is expected to increase in future decades (Ikonen et al. 2014). Vessel passage through icy waters entails exposure to additional ice-related loads on the propulsion system. Ice-related loads furthermore affect the efficiency and safety of vessel operations (Polić et al. 2014) and could result in failure of other shaft line elements if not accounted for. A study by the Transportation Safety Board of Canada (2010) found that propulsion system failure is still one of the greatest contributors to vessel failure.

Shaft-line components, including the propeller, are therefore required to operate efficiently in ice and open water while withstanding both extreme loads and fatigue loads (Huisman et al. 2014). Extreme and cyclic moderate loading of the propeller is increased during propeller-ice interaction. Extreme loading dictates the ultimate strength of propeller design and cyclic moderate loading determines the fatigue life of the propeller (Huisman et al. 2014). These loads are transmitted to other shaft-line elements which should not deform plastically in the event of propeller failure. The propeller and shaft line elements of ice going vessels are exposed to transient torsional and axial vibration induced by propeller-ice interaction which

leads to the interest in the effect of ice loads on propulsion designs (Batrak et al. 2014).

During both full-scale trials and model-scale investigations, ice-related propeller loads are typically measured between the engine and the propeller on the shaft (Polić et al. 2014). These loads are not measured directly and include the dynamic response of the mechanical transmission components (Polić et al. 2014). The use of numerical methods is useful to predict the global loads at the propeller but is not adequate to optimize the efficiency and reliability design of the propeller (Huisman et al. 2014). Tang & Brennan (2013) recommend that multi-point measurements are more reliable than conventional single measurements, especially for shaft lines containing highly flexible components. To date, there exists no in-depth, definitive study on propeller-ice interaction (Sampson et al. 2009) and there is a lack of knowledge regarding the physical processes during propeller-ice interaction which cause ice-loading (Huisman et al. 2014).

Shipping registers, such as Korean Register (Korean Register 2015), American Bureau of Shipping (American Bureau of Shipping 2006), Det Norske Veritas (Det Norske Veritas 2011a) and Lloyd's Register (Germanischer Lloyd 2007) specify the requirement for calculation of torsional shaft line vibration during the design stage. Full-scale measurements are subsequently performed during sea trials in order to ensure safe vessel operation (Tang & Brennan 2013). Although full-scale measurements are time-consuming and costly, such measurements offer advantages over a model-scale approach. The design and extensive calibration of a model test rig is avoided (Brouwer et al. 2013). Furthermore, full-scale measurements of vessels provide accurate performance data of the vessel relative to the environmental conditions (Dinham-Peren & Dand 2010).

It is required to design the propulsion line components with sufficient strength to withstand the maximum induced loads on the propeller. At the same time, damage to other propulsion line components is to be prevented in the event of plastic bending of a propeller blade (Det Norske Veritas 2011a). A further requirement is that fatigue strength is to accommodate the load distribution as shown in Eq. 1 (Det Norske Veritas 2011a):

$$Q_A(N) = Q_{A,max}\left[1-\frac{log(N)}{log(ZN_{ice})}\right]^{1/k_w}_{[Nm]} \quad (1)$$

where Q_A is the response torque amplitude on the shaft during a sequence of ice impacts on the propeller and $Q_{A,max}$ is the highest response torque amplitude on the shaft during a sequence of ice impacts on the propeller. N_{ice} is the number of ice impacts, N is the number of cycles analyzed and Z is the number of propeller blades. The Weibull shape parameter is assumed to have a value of $k_w = 1$ (Det Norske Veritas 2011a).

Cycle counting is a convenient method to summarize irregular loading histories by determining the number of times certain cycles of various magnitudes occur (ASTM International E1049-85 2011). Many different cycle counting methods, of which level-crossing counting, peak counting, simple-range counting and rainflow counting are the most well-known (ASTM International E1049-85 2011). Of these methods, rainflow counting has been proven to be the better method for irregular loads (Connor et al. 2010). Rainflow counting was also used by Myklebost & Dahler (2013) during the analysis of shaft line torque. Rainflow counting enables one to extract cycles from randomly loaded data, with amplitudes defined as half the difference between two consecutive peaks and troughs.

Vessel propulsion systems are exposed to a wide spectrum of loads during operation. Only

the dominating cases are considered during fatigue analysis as loads below the Mean Continuous Rating (MCR) in bollard condition theoretically do not result in shaft line failure, with MCR defined as the maximum rated torque Q_{MCR} the propulsion system can safely operate at continuously (Det Norske Veritas 2011a).

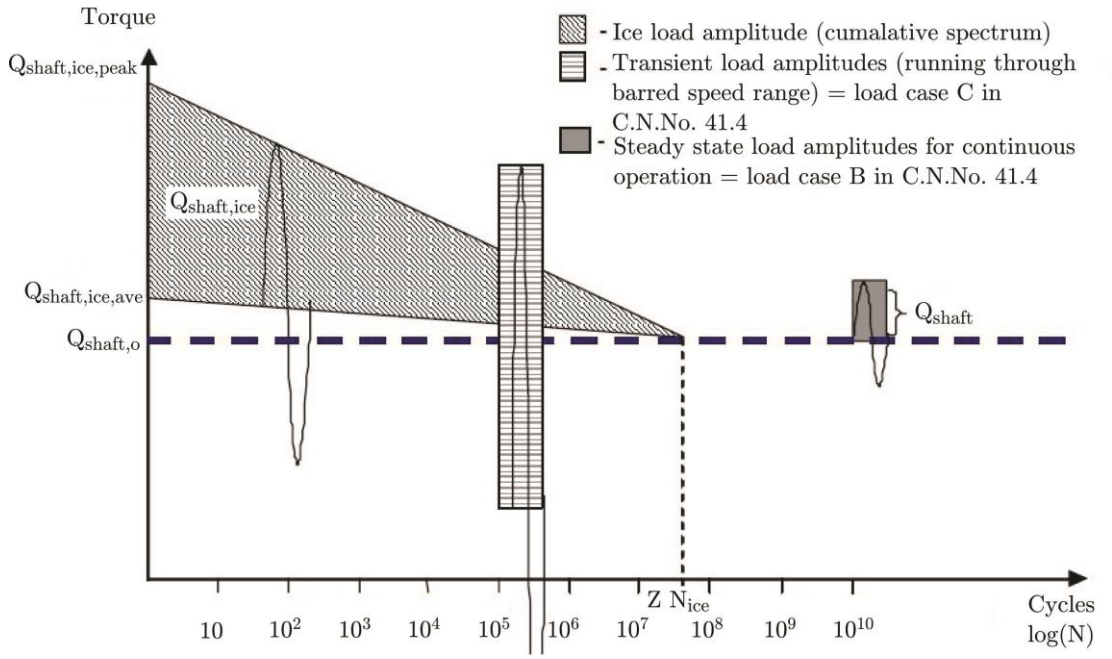

Figure 1. Typical load cases to be assessed for directly coupled two-stroke plant ice class vessels. Adapted from (Det Norske Veritas 2011a)

Figure 1 represents the typical load cases that need to be assessed for vessels navigating in ice with a directly coupled two-stroke plant. $Q_{shaft,ice,peak}$ is the maximum response peak torque measured in the shaft due to ice impacts on the propeller, $Q_{shaft,ice,ave}$ is the average torque in the shaft during an ice milling sequence, $Q_{shaft,o}$ is the shaft torque at maximum continuous power in bollard condition, $Q_{shaft,ice}$ is the response torque in the shaft due to ice impacts on the propeller and Q_{shaft} is the total torque response in the shaft due to external loading on the propeller.

In light of the sparsity of public domain operational data, full-scale measurements of axial- and shear strain on two polar research vessels were undertaken. Measurements on the shaft-line have a two-fold purpose: Firstly, to obtain an indication of the transient torque and thrust in the shaft and secondly, to provide a means through which propeller loads can be estimated by inverse methods (Ikonen et al. 2014). The present study focuses on the former purpose, whereby the operational loading on the propulsion components is to be informed and compared to existing ice class rules (Det Norske Veritas 2011b). The proportional time of vessel activities is categorized from response data. Rainflow counting is performed on the transient thrust and torque histories which are calculated from strain measurements for each operational category. The measurement data is extrapolated over the full voyage durations and this information is subsequently used to predict the operational load profiles for the investigated vessels.

FULL-SCALE MEAUREMENTS

Vessel Descriptions

The SAA II, depicted in Figure 2, was manufactured in Rauma shipyard in 2012 by STX Finland (Bekker et al. 2014). The hull was strengthened in accordance with DNV ICE-10 and the vessel classified to Polar Ice Class PC-5 (Bekker et al. 2014). She is therefore rated for year-round operations in medium first-year ice containing old ice inclusions (International Association of Classification Societies 2011). The ship is propelled by four 3 MW diesel generators which power two Conver Team electric motors of 4.5 MW each. She is equipped with two four-bladed variable pitch propellers with individual shaft lines (STX Finland Oy 2012).

Figure 2. SAA II vessel instrumented for the 2015/2016 relief voyage Antarctica.

Figure 3. The FS Polarstern was instrumented for the PS-100 Arctic voyage, 2016.

The FS Polarstern (Figure 3) was manufactured in 1982 by Howaldtwerke-Deutsche Werft AG in Kiel and outfitted by Werft Nobiskrug GmbH in Rendsburg (Grobe & Alfred Wegener Institute 2007). The hull was strengthened in accordance with Germanischer Lloyd Ice Class E3, which is the equivalent of Polar Ice Class PC-5 (Transport Safety Agency 2010). Her propulsion design comprises four diesel engines, each 3.5 MW, which in turn powers two shaft lines with four-bladed variable pitch propellers.

A key difference between the FS Polarstern and the SAA II is that the SAA II has open propellers and a direct diesel to electric drive to the shaft line as shown in Figure 4. The FS

Polarstern design includes ducted propellers (*Figure 5*) as well as a direct diesel engine drive through a gearbox. Principal specifications of the vessels are presented in Table 1.

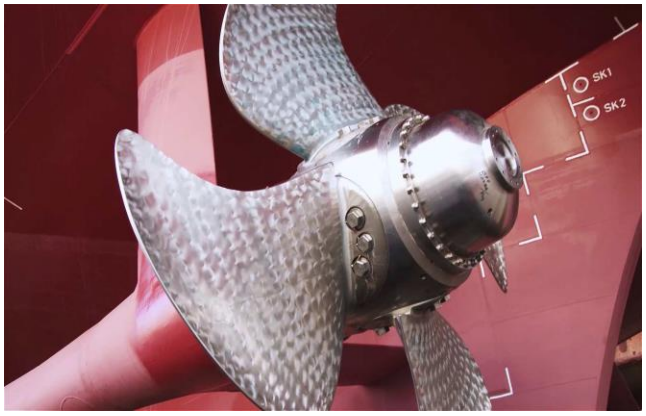

Figure 4. The four-bladed propeller of the SAA II.

Figure 5. The FS Polarstern has a ducted propeller design.

Table 1. Vessel specifications (STX Finland Oy, 2012; The Alfred Wegener Institut, 2016).

	SA Agulhas II	FS Polarstern
Gross tonnage	12 897 tons	12 614 tons
Length / Breadth	134 m / 22 m	118 m / 25 m
Classification	Det Norske Veritas	Germanischer Lloyd
Class notation	1A1 PC-5/ICE-10	100 A5 ARC 3
Yard	STX Finland, Rauma, Finland	Howaldtswerke-Deutsche, Hamburg & Kiel, Germany
Year built	2012	1982
Main engine maker	Wärtsilä	Klöckner-Humboldt-Deutz
Diesel engine type	6L32	KHD RBV 8 M 540
Electric motor type	N3 HXC 1120 LL8	-
Speed / Power at MCR	140 rpm / 4500 kW	182.4 rpm / 7765 kW
Nominal torque	307 $k \cdot Nm$	407 $k \cdot Nm$
Propeller maker	Rolls-Royce	Vereinigte Edelstahlwerke
No. of blades / Diameter	4 / 4.3 m	4 / 4.2 m
Shaft characteristics	Direct drive	1:3.563 gearbox ratio
No. of motors / propellers	2 / 2	4 / 2

Arctic and Antarctic Voyages

The global positioning system (GPS) track of the 2015/2016 Antarctic relief voyage of the SAA II presented in Figure 6(a). The vessel departed Cape Town Harbour (1) and headed south along the Greenwich Meridian. Ice was encountered prior to reaching the ice shelf at

Penguin Bukta (3). From here the vessel departed for Akta Bukta near the German Antarctic Research Station, Neumayer and continued through heavy pack ice towards the South Sandwich Islands towards South Thule (4). She exited the ice field and reached South Georgia (5) and returned to Penguin Bukta (3) before heading back to Cape Town (1).

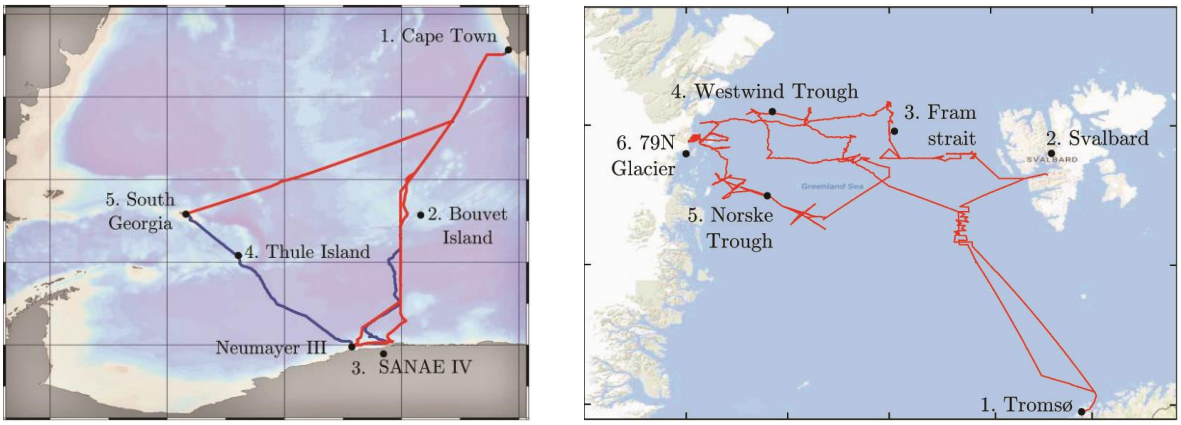

(a) Antarctic voyage (b) Arctic voyage

Figure 6. Round voyages for (a) SAA II to Antarctica (Red - outbound, blue - return voyage) and (b) FS Polarstern to the Arctic. Background for Antarctica adapted from AWI (2015) and for Arctic from Google (2016).

For the PS-100 Arctic voyage on-board the FS Polarstern (Figure 6(b)) the FS Polarstern departed from Tromsø (1), Norway and sailed for Longyearbyen, Svalbard (2). From there she headed West North West towards the zero degree meridian and sailed along the Fram Strait (3). Ice was encountered during navigation along the zero meridian to just below 81 degrees North. The voyage continued Westwards towards the West wind Trough (4) where ice cover was less concentrated. The ship re-entered open water on her southerly journey to the Norske Trough (5) where she re-encountered significant ice cover. She proceeded towards the 79 North Glacier (6) at Greenland before exiting the ice filed and returning to Tromsø (1). The total duration of the voyage was 51 days, of which an estimated 70 hours was spent navigating in thick Arctic ice.

Instrumentation

Strain gauges were installed on the port side shaft lines of each of the SAA II and FS Polarstern to determine the shear and axial strain. This allows for the determination of the instantaneous torque and thrust at the measurement locations. For shear strain measurements T-rosette gauges were installed at a 45° angle to the shaft mid-plane in a Wheatstone bridge configuration. Figure 7(a) provides a diagram of the Wheatstone bridge layout, indicating the supply voltage, U_E, and output voltage, U_A, as well as the strain gauge resistances (R_1 to R_4) for the four gauges in a full bridge. Figure 7(b) depicts the orientation of the strain gauges for shear strain measurement on the shaft. The bridge was set up to reject both axial- and bending strain whilst compensating for temperature variations.

A further set of T-rosette strain gauges were installed on either side of the shaft line to enable axial strain measurements. These gauges were oriented parallel to the shaft mid-plane as shown in Figure 7(c). The full bridge configuration is robust for axial strain measurement as it is compensated for temperature variation and bending strain.

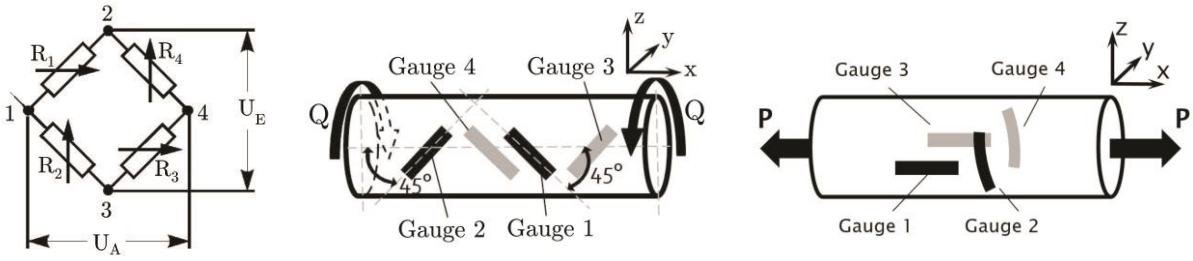

Figure 7. Strain gauge placement on shaft for (a) torque and (b) thrust measurements. Adapted from Hoffmann (Hoffmann 2001).

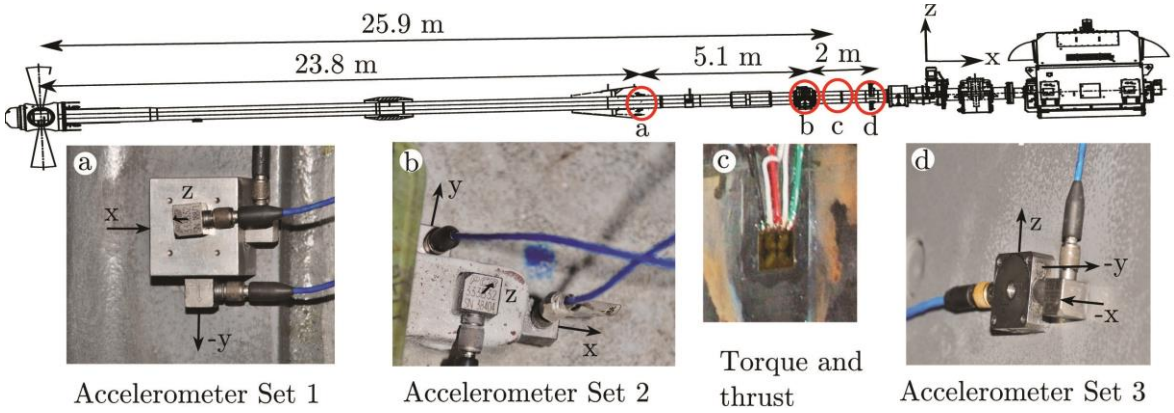

Figure 8. Accelerometers and strain gauges mounted along the shaft line for the SAA II (Adapted from technical ship drawings (STX Finland Oy 2012))

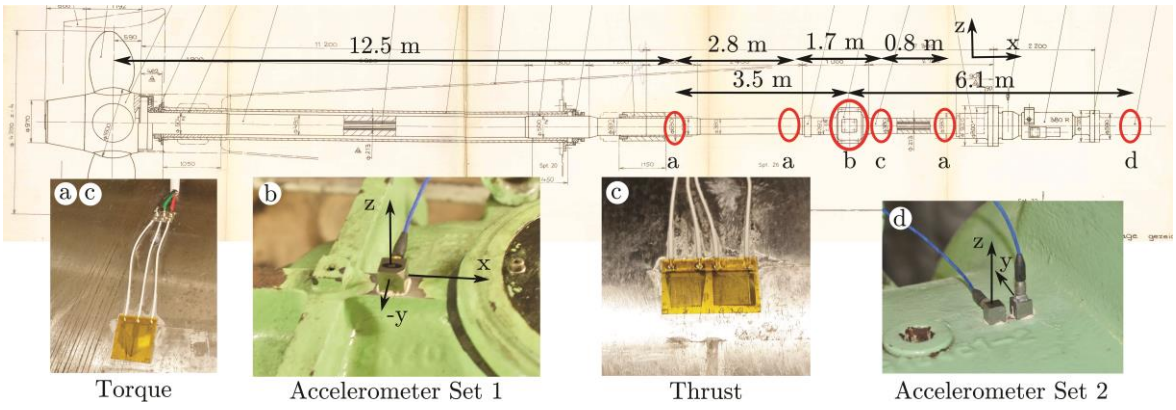

Figure 9. Accelerometers and strain gauges mounted along the shaft line for the FS Polarstern (Adapted from technical ship drawings (Werft Nobiskrug GmbH 1980))

The strain gauge installations on the SAA II were located at 25.9 m inboard from the centre of gravity of the port side propeller as shown in Figure 8. The measurements were wirelessly transmitted via wi-fi from a V-link system to a WSDA-Base data gateway, managed through Node Commander software. Data was acquired with a Hottinger Baldwin Messtechnik (HBM) acquisition system. In addition, three accelerometer sets (PCB, 100 mV/g) were mounted at three locations on the shaft support structures. The orientations of the accelerometers are indicated in Figure 8. Data was acquired through a HBM Quantum mobile data acquisition system and transmitted to a laptop via an ethernet cable and recorded through Catman AP V3.5 software at a sample rate of 600 Hz.

Similar measurements were performed on the FS Polarstern as shown in the instrumentation

layout presented in Figure 9. The power source in the shaft line room originated directly from the generator, resulting in unstable power. Two sets of accelerometers were installed on the FS Polarstern on the available shaft support structures within the intermediate shaft line room. One x-direction (fore-aft) measurement was recorded as the bearings on which accelerometer measurements were performed are radial bearings that do not transfer axial vibration well.

METHODS

Calculation of Shaft Line Torque and Thrust

The torque in the shaft can be determined from the output voltage of the Wheatstone bridge through:

$$Q_{shaft} = U_A \frac{\pi E(d_o^4 - d_{in}^4)}{16 U_E k d_o (1+\nu)}_{[Nm]} \tag{2}$$

Here, E is the Young's modulus, ν is the Poisson's ratio and d_o and d_{in} respectively reflect the outer and inner diameters of the hollow shaft. The strain gauge factor, k, is directly obtained from manufacturer specifications. The thrust was calculated from the T-rosette Wheatstone bridge output voltage with Eq, (3):

$$T_{shaft} = \frac{U_A E \pi (d_o^2 - d_{in}^2)}{2 U_E k (1+\nu)}_{[N]} \tag{3}$$

Table 2. Shaft line dimensions, material properties and shaft related variables for measurement location (STX Finland Oy 2012; Rolls-Royce AB 2010; Escher Wyss 1980; Metallurgica Veneta 2004; Det Norske Veritas 2011a).

Description	Symbol	SA Agulhas II	FS Polarstern
Modulus of elasticity	E	210 GPa	220 GPa
Shear modulus	G	81 GPa	84 GPa
Outer diameter	d_o	0.5 m	0.39 m
Inner diameter	d_{in}	0.175 m	0.213 m
Hub diameter	d_h	1.32 m	1.60 m
Maximum ice thickness	H_{ice}	2.0 m	2.0 m
Ice strength index	S_{ice}	1.1 m	1.1 m
Pitch at $0.7 \cdot$ radius	$P_{0.7}$	5.15 m	4.42 m
Expanded blade area ratio	EAR	0.51	0.55
Depth of propeller centerline	h_o	3.75 m	6.92 m

The shaft line dimensions for the SAA II were obtained from engineering drawings by (STX Finland Oy 2012). The material specifications were sourced from manufacturer documentation (Rolls-Royce AB 2010). Polarstern shaft line dimensions were sourced from engineering drawings by (Werft Nobiskrug GmbH 1980) and the material properties from a test certificate of materials (Germanischer Lloyd 1981). As the FS Polarstern was built in

1982, old German material specifications were used. The current equivalent classification was obtained from a catalogue (Metallurgica Veneta 2004), in which the new material grade equivalent for St52-3N was found to be S355J2. The dimensions, material properties and shaft related variables for the two vessels are presented in Table 2. The depth of the propeller centreline, h_o, was not directly obtainable and was extracted by scaling a measurement from the vessel drawings.

Determination of Representative Loading Profiles

As data recordings were not possible throughout the voyages, it was required to classify vessel activities along with their associated load histories from the recorded data. This was achieved by categorizing the data into three categories namely: open water, ice navigation and stationary vessel operations. The appropriate categories could be determined by consideration of the vessel location, speed, shaft line data and logbook information. Vessel operations are recorded in the ship logbooks which assisted with the determination of stationary periods. The boundary between ice navigation and open water operational categories was more difficult to distinguish precisely as low ice concentrations and thickness do not prominently affect the shaft line response. The threshold between ice and open water navigation was distinguished based on three indicators: i.) By classification of the corresponding data in accordance with continual ice observation records from the bridge. ii.) Investigation of the shaft line torque and thrust, which showed a more oscillatory, higher amplitude response in ice compared to open water. iii.) Vessel speed is commonly reduced during navigation in thick ice.

Rainflow Counting

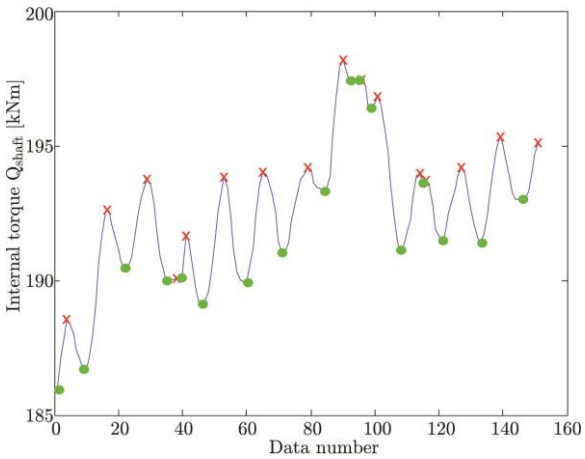

Figure 10. The identification of peaks(crosses) and troughs (circles) by the `sig2ext.m` (Nieslony 2003) algorithm.

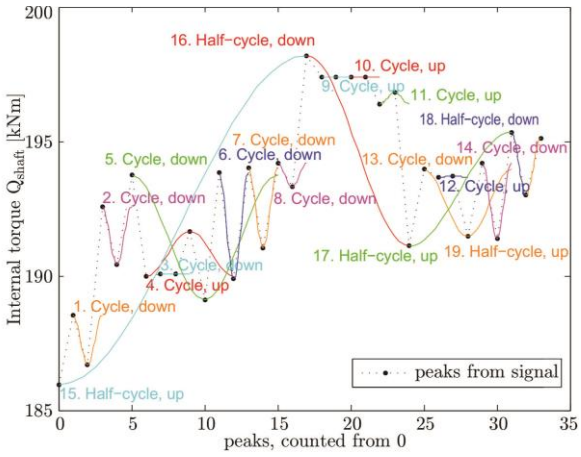

Figure 11. A diagram which demonstrates the extraction of loading cycles by the `rainflow.m` (Nieslony 2003) algorithm.

Rainflow counting involved peak and cycle counting on the calculated torque (Eq.1) and thrust (Eq. 2) from shaft line measurement data of the two vessels. The local maxima and minima (turning points) of the signals were first identified using a MATLAB algorithm, `sig2ext.m` (Nieslony 2003). A graphical result for a half second time signal is presented in Figure 10 where red crosses indicate the peaks and green dots the troughs, which were identified by the algorithm. To obtain the amplitudes of the data signals, the identified

maxima and minima are processed by a second algorithm `rainflow.m` (Nieslony 2003) which extracts and counts the identified cycles as demonstrated in Figure 11.

RESULTS

Vessel Loading Profiles

The total time spent in ice, open water and stationary operations was determined for each voyage as shown in Figure 12 and Figure 13. The actual duration was compared to the time of the available full-scale recordings to determine scaling factors for the estimation of the expected load profile for each vessel (Table 3).

Table 3. Duration of voyage spent in open water, ice and stationary with recorded times for each of these conditions.

	SA Agulhas II			FS Polarstern		
	Actual [days]	Recorded [days]	Scaling factor [days]	Actual [days]	Recorded [days]	Scaling factor [days]
Ice navigation	10.67	8.54	1.25	11.69	9.15	1.27
Open water	39.96	5.42	7.38	17.31	5.03	3.44
Stationary	17.46	1.58	11.03	19.97	10.95	1.82
Total	68.09	15.54	4.38	48.97	25.13	1.95

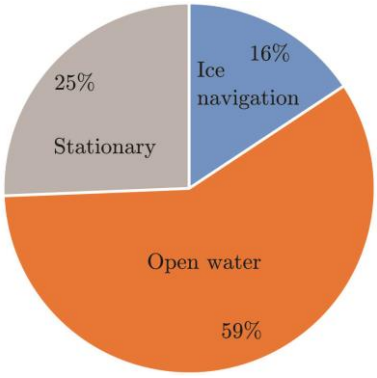

Figure 12. A classification of the activities of the SAA II during the 2015/2016 Antarctic voyage.

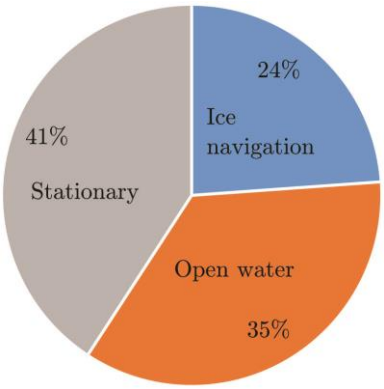

Figure 13. A classification of the activities of the FS Polarstern for the PS-100 voyage to the Arctic, 2016.

Rainflow Counting

Rainflow counting analyses of peak torque values are presented in Figure 14 for both vessels. The plots only include significant peaks, as there are many high magnitude peaks occurring at low cycle magnitudes. The highest peak values and total cycles recorded during these conditions are presented in Figure 16. The bin size for the histograms was selected to be 1 kN·m for torque and 1 kN for thrust. When comparing the results from the operational categories for the two vessels, the following was observed for ice navigation in Figure 14 (a) and (b):

i.) Ice navigation results in higher peak values, with the SAA II having a higher distribution overall.

ii.) The most peak torsional loads in ice occurred around 100 kN·m for the SAA II and around 60 kN·m and 80 kN·m for the FS Polarstern.

iii.) During ice navigation both vessels display a secondary region of increased loading cycles at higher torque magnitudes of 310 kN·m for the SAA II and 250 kN·m for the FS Polarstern, whereby these high magnitude peaks were not as evident in open water or stationary operations.

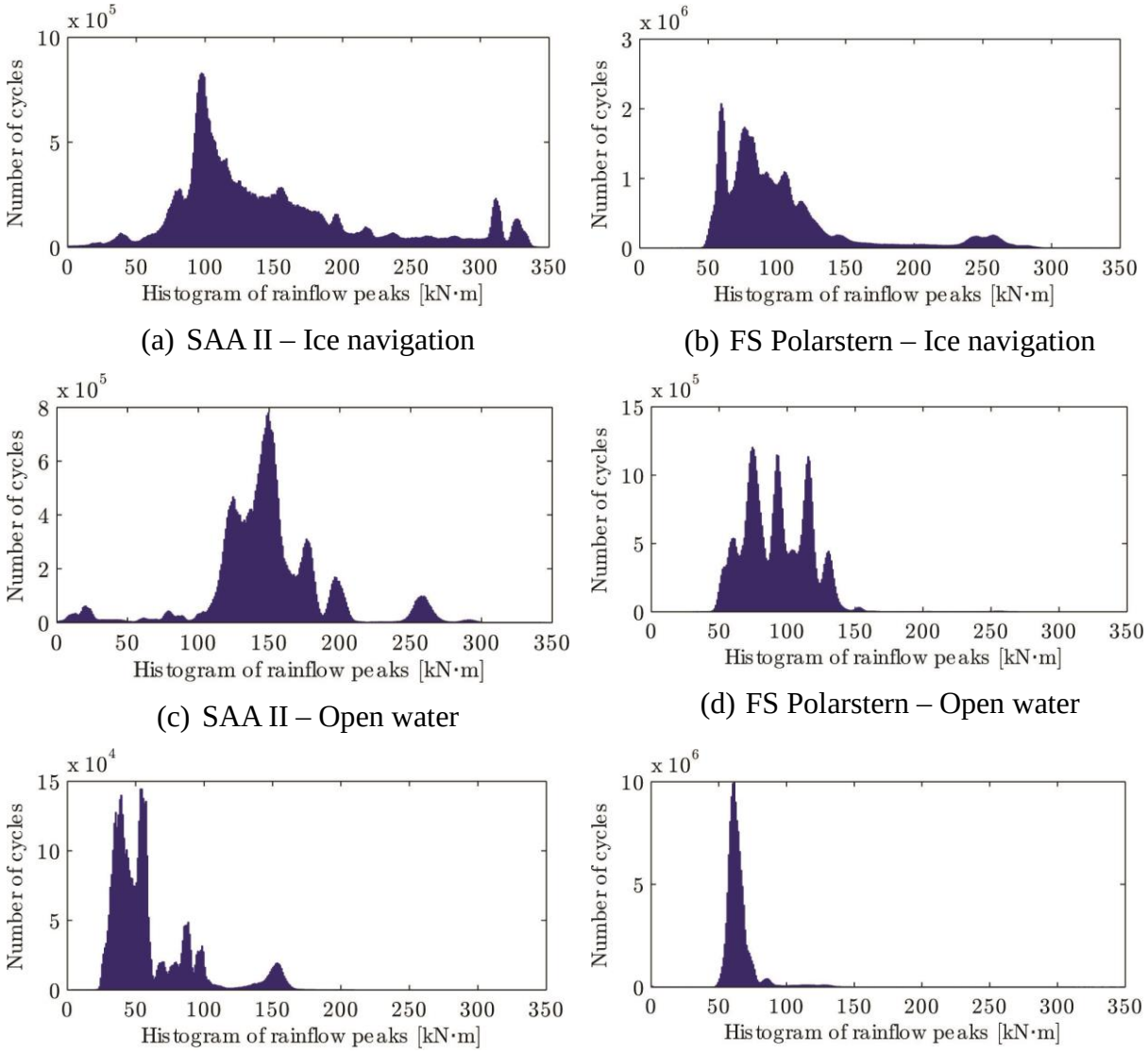

(a) SAA II – Ice navigation

(b) FS Polarstern – Ice navigation

(c) SAA II – Open water

(d) FS Polarstern – Open water

(e) SAA II - Stationary

(f) FS Polarstern – Stationary

Figure 14. Comparison of torque peak rainflow cycles for the SAA II (left) during the 2015/2016 Antarctica voyage and for the FS Polarstern (right) during the 2016 Arctic voyage.

Rainflow counting for open water passage in Figure 14(c) and (d) show that:

i.) The greatest number of torque peak cycles for the SAA II occurred at 150 kN·m which amounts to more cycles at a higher cycle count than for ice navigation. This is explained by considering that the pitch of the propeller and shaft line speed is lowered during ice navigation to reduce the speed of the vessel while maintaining enough torque on the shaft

line to allow the propeller to chop through ice. In open water, the SAA II generally operated above 7 knots at a pitch of 87% and shaft line speed of 135 rpm, compared to a speed below 6 knots, pitch of 74% and shaft line speed of between 90 and 110 rpm during ice navigation.

ii.) The high cycle loading just above 250 k·Nm could be a result of vessel operations just shy of the maximum pitch of 99.5% in open water conditions upon the return leg from Antarctica to Cape Town.

iii.) The FS Polarstern data presented a much narrower spread of high cycle peak torque values, ranging from 50 to 150 k·Nm. Within this range there were three distinct high cycle peaks, which were also apparent for ice navigation condition. The FS Polarstern generally operated below 7 knots during ice navigation, however the shaft line speed remained relatively constant around 174 rpm throughout the voyage, as they were directly driven by the diesel generators.

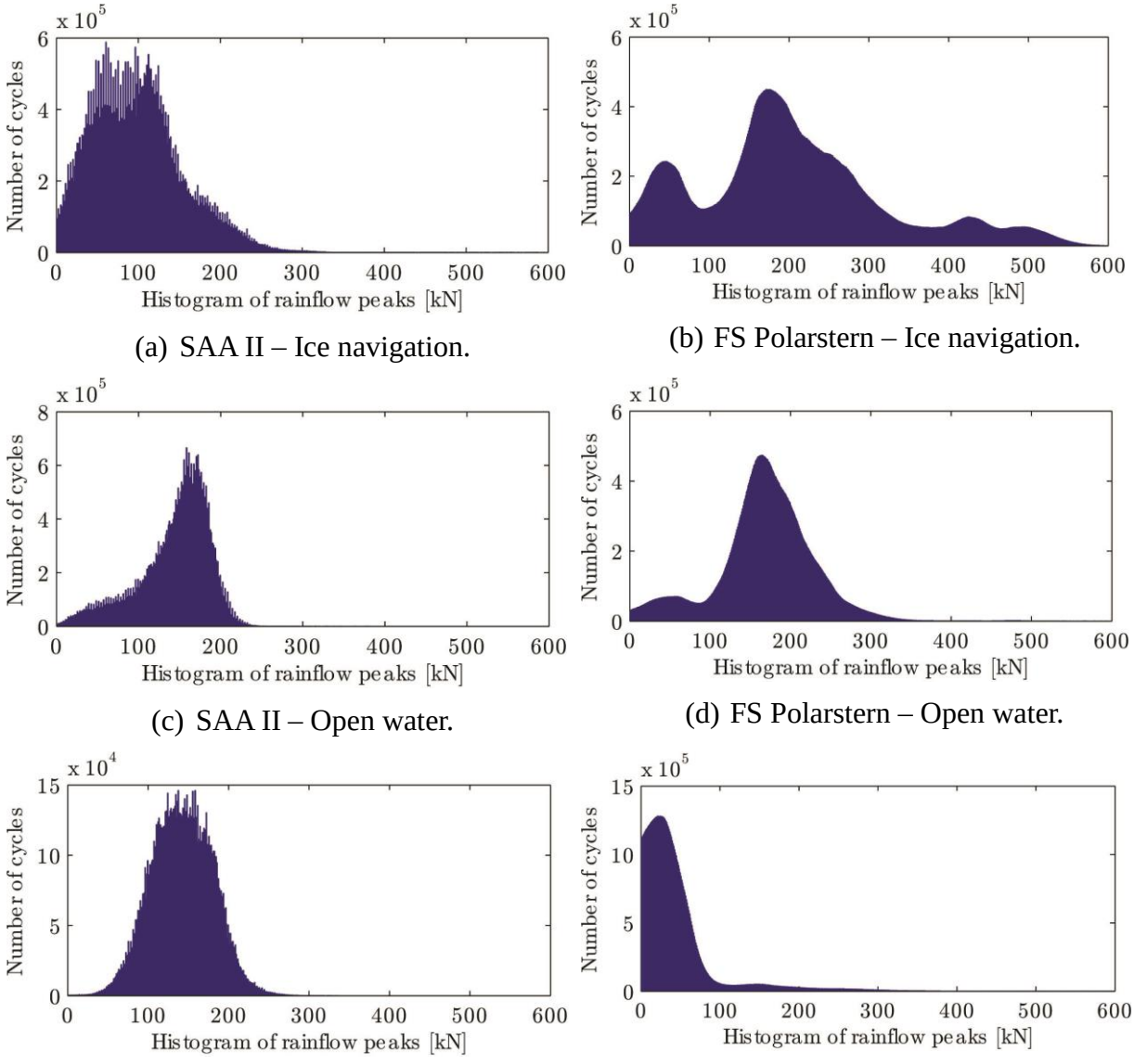

(a) SAA II – Ice navigation.

(b) FS Polarstern – Ice navigation.

(c) SAA II – Open water.

(d) FS Polarstern – Open water.

(e) SAA II - Stationary

(f) FS Polarstern – Stationary.

Figure 15. Comparison of thrust peak rainflow cycles for the SAA II (left) during the 2015/2016 Antarctica voyage and for the FS Polarstern (right) during the 2016 Arctic voyage.

For the stationary case (Figure 14(e) and (f)):

i.) Low torque peak cycles are evident as the pitch of the propeller was set to approximately zero during these conditions.

i) The maximum cycles for the FS Polarstern occur above 50 kN·m. This could be due to the direct diesel engine drive which induces a torque greater than 50 kN·m, whereas the SAA II has a direct electric drive which is not subjected to gearbox and combustion engine vibrations.

There are several high peak torque cycles evident for the stationary case for both vessels. The vessels use their respective propellers to operate on station during deployment of equipment overboard or retaining constant thrust on the propeller to maintain the vessel stationary against the shelf or bay ice. Histograms of the rainflow counting analyses of thrust peaks are presented in Figure 15. The following observations were made:

i.) The FS Polarstern experienced a greater range of significant thrust loading peaks during ice navigation, ranging from 0 to 600 kN.

ii.) The largest number of cycles for the FS Polarstern shaft occurred at 180 kN for both ice and open water conditions and at 25 kN for the stationary conditions.

iii.) For the SAA II, the largest cycles were distributed between 50 and 150 kN for the ice condition, 170 kN for the open water condition and 140 kN for the stationary condition.

iv.) The reason for the larger significant peaks during open water compared to ice navigation is attributed to the greater propeller pitch under these conditions.

The maximum bin size for each operational category is presented in Figure 16 from which it is evident that the FS Polarstern measurements presented greater torque peaks, torque amplitudes and thrust amplitudes during the stationary condition compared to the open water condition. This is explained by the incidence of rapid shaft line loading during stations whereby the vessel is required to remain positioned in the same location. Such operations often require pushing back against floe ice.

The FS Polarstern experienced higher peak loads compared to the SAA II. This could be due to the Arctic containing harder, multi-year ice compared to the Antarctic. Alternatively the design of the FS Polarstern induces higher loads compared to the SAA II due to shaft line geometry. The location of measurements along the shaft is also a factor as torque fluctuates throughout the shaft. For a fair comparison of load conditions shaft line loads need to be converted to propeller loads through inverse methods (Ikonen et al. 2014) whereby ice induced loading on the propeller could be compared.

The predicted load profiles, which were derived from the three operational categories, are compared in Figure 17 on logarithmic scales. The torque peak values were divided by the nominal rated torque, Q_{MCR}, to obtain the load response factor, K_a which is used for vessels exposed to varying loads. This allows for the safe loading on components along the shaft line, specifically the propeller, to be determined.

Raw load response data typically exhibits a change in slope of which the cause is ascribed to one of two possibilities Myklebost & Dahler (2013): either the statistical distribution differs from medium to high impact values, or the distribution below the change in slope is a result of control system or motor excitations and the distribution above the change in slope is as a result of propeller-ice impacts. This corresponds to the typical load cases in Figure 1 (Det Norske Veritas 2011a) in which ice load amplitudes occur above the distinct change in slope.

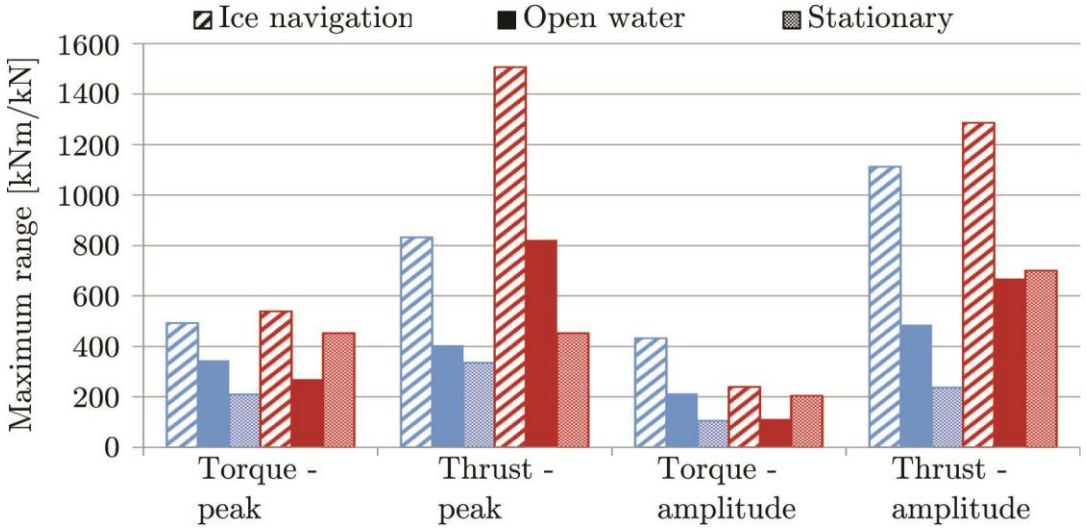

Figure 16. Maximum recorded bin size for the SAA II (blue) and FS Polarstern (red).

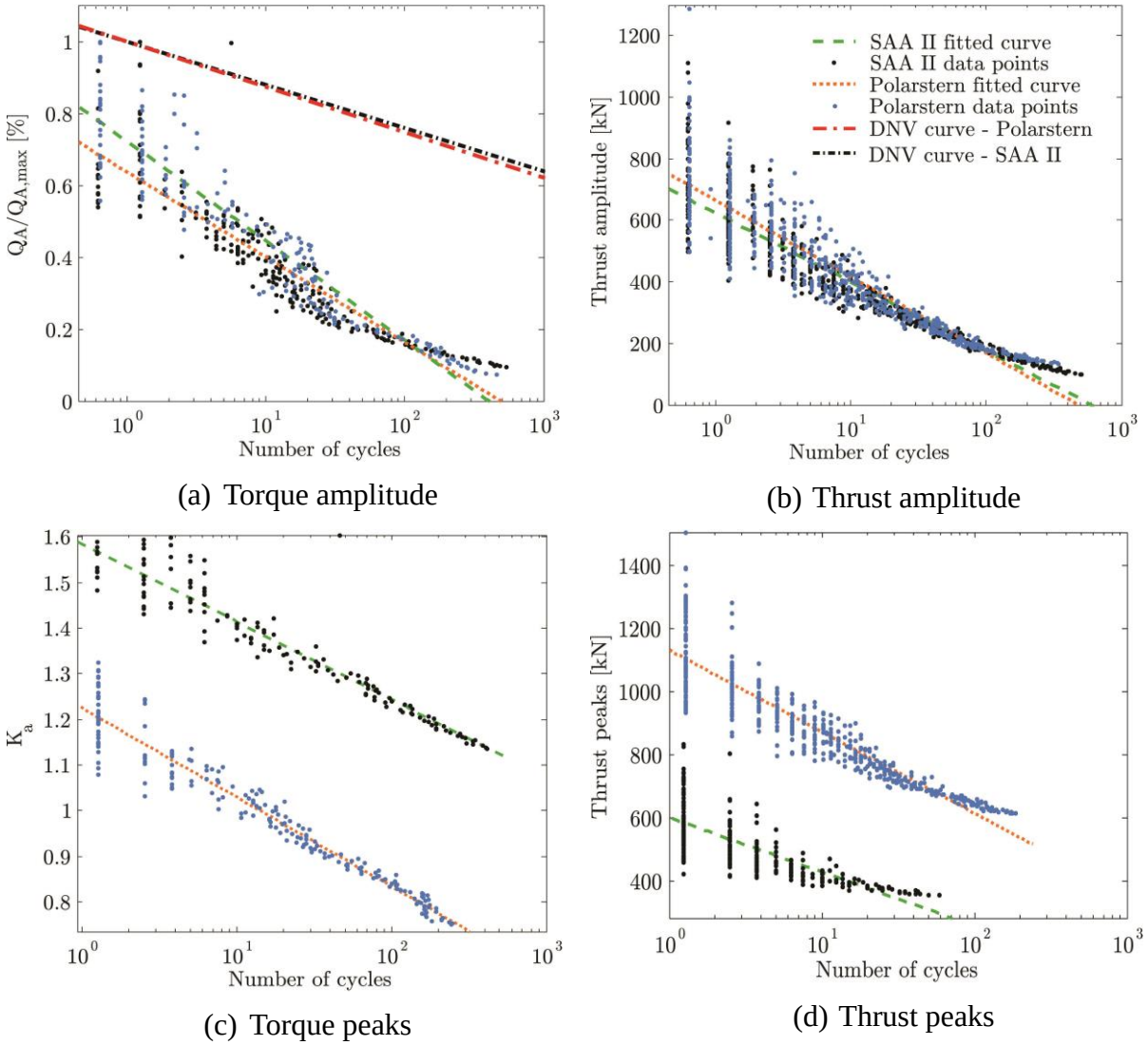

(a) Torque amplitude

(b) Thrust amplitude

(c) Torque peaks

(d) Thrust peaks

Figure 17. Comparison between two vessels of predicted load profiling during a voyage to the Arctic and Antarctica.

DNV (Det Norske Veritas 2011a) provide a relationship to predict the cumulative shaft torque distribution Eq.(1) through torque amplitudes as a function of N_{ice}. This equation was presented as an accumulated load spectrum in Figure 17 (a). To obtain this curve, the procedures described in the DNV ice rules (Det Norske Veritas 2011b) were used with variables from Table 2. These curves are presented in Figure 17(a) for the SAA II and the FS Polarstern. The representative curves for the thrust and torque peak and amplitude analyses are recorded in Table 4, with regression values and total cycles for each of the four cases for each vessel.

Table 4. Regression, total cycles and curve fit equations for rainflow counting data of the form $y = A\log x + B$.

	A	B	R^2	Total cycles
SAA II				
Torque amplitude	-102.47	275.81	0.82	8.73×10^7
Torque peak	-0.17	1.58	0.90	8.72×10^7
Thrust amplitude	-223.87	623.52	0.86	1.27×10^8
Thrust peak	-171.93	600.08	0.60	1.24×10^8
DNV curve	-0.12	1		
FS Polarstern				
Torque amplitude	266.41	173.21	0.89	2.72×10^8
Torque peak	-0.20	1.22	0.94	2.72×10^8
Thrust amplitude	-249.58	665.97	0.83	2.63×10^8
Thrust peak	-258.60	1131.57	0.85	2.21×10^8
DNV curve	-0.13	1		

Myklebost & Dahler (2013) determined that this change in slope occurred at $1.4\cdot Q_{MCR}$ during the 2012/2013 voyage for the SAA II. For the 2015/2016 voyage, it was determined to be $1.14\cdot Q_{MCR}$ for SAA II and $0.75\cdot Q_{MCR}$ for the FS Polarstern during the 2016 PS-100 voyage. The change in slopes for peak torque, peak thrust, torque amplitude and thrust amplitude were determined and the data above these points presented in Figure 17. This was done to focus the analysis on the ice related loads. The following observations are made from Figure 17:

i.) The SAA II experienced greater torque peaks relative to Q_{MCR}, however similar magnitudes were experienced by the two vessels overall. The plot is deceiving as it appears the SAA II experienced greater torque peaks. This is due to the 100 kN·m difference between the Q_{MCR} of the two vessels.

ii.) Significantly smaller thrust peaks were experienced by the SAA II throughout its voyage compared to the FS Polarstern. One possible reason could be the smaller diameter shaft of the FS Polarstern, thus experiencing a greater thrust value at the location of the strain gauge measurement.

CONCLUSIONS

Through rainflow counting analyses, the cyclic torsional and thrust loading of two polar vessel shaft lines have been highlighted for operations in open water, ice and stationary work. In the Arctic, the FS Polarstern was exposed to much greater thrust peaks in comparison to the SAA II, during her Antarctic voyage. Comparison of the peak torque cycles of the two vessels showed that the SAA II experienced greater torque peaks relative to its MCR compared to the FS Polarstern. The two vessels did however experience the same order of magnitude peak torques during their respective voyages. This does not necessarily imply that vessels operating in the Arctic and Antarctica will be exposed to the same magnitude of peak torque. Shaft geometry and measurement location do influence the obtained dynamic responses. An objective comparison would include inverse force estimation to eliminate the dynamic response of the shaft and propulsion components and subsequent comparison of the applied ice loads at the propeller. This analysis does however emphasize the importance of shaft line torsional analysis, which could identify the operation of the vessels above its MCR.

ACKNOWLEDGEMENTS

The financial assistance of the National Research Foundation (NRF) towards this research is hereby acknowledged. Captain Gavin Syndercombe and the SMIT Amandla crew and Kapitän Stefan Schwarze and his crew on-board the Polarstern is appreciated during the respective Antarctic and Arctic voyages. The collaboration of Aalto University, Finnish Meteorological Institute, the Alfred-Wegener-Institut and the Department of Environmental Affairs of South Africa is gratefully acknowledged.

REFERENCES

American Bureau of Shipping, 2006. Guidance notes on ship vibration.

ASTM International E1049-85, 2011. ASTM E1049-85: Standard practices for cycle counting in fatigue analysis. *Designation: E1049 - 85*.

Batrak, Y.A., Serdjuchenko, A.M. & Tarasenko, A.I., 2014. Calculation of torsional vibration responses in propulsion shafting system caused by ice impacts. *Torsional Vibration Symposium*, (January 2011).

Bekker, A. et al., 2014. OMAE2014-24128. In *ASME 33rd International Conference in Ocean, Offshore and Arctic Engineering*. San Francisco, California, USA.

Brouwer, J., Hagesteijn, G. & Bosman, R., 2013. Propeller-ice impacts measurements with a six-component blade load sensor. In *Third International Symposium on Marine Propulsors*. Tasmania, pp. 47–54.

Connor, S.O. et al., 2010. Fatigue life monitoring of metallic structures by decentralized rainflow counting embedded in a wireless sensor network. In *Proceedings of the ASME 2010 Conference on Smart Materials, Adaptive Structures and Intelligent Systems*. Philadelphia, PA, USA.

Det Norske Veritas, 2011a. Classification of ships for navigation in ice. *Rules for Classification of Ships*, 5(1322), pp.1–142.

Det Norske Veritas, 2011b. Ice strengthening of propulsion machinery. *Classification Notes*, 1(51).

Dinham-Peren, T. & Dand, I., 2010. The need for full scale measurements. In *William Froude Conference: Advances in Theoretical and Applied Hydrodynamics - Past and Future*. Portsmouth. Available at: http://media.bmt.org/bmt_media/resources/33/RINA Froude Conf - The Need for Full Scale Measurements.pdf.pdf.

Escher Wyss, 1980. Gesamtanordnung VP Anlage.

Germanischer Lloyd, 2007. Rules for classification and construction. *Part 6 Offshore Technology, Chapter 5 Machinery Installations, Section 7 Torsional Vibrations*.

Germanischer Lloyd, 1981. Test certificate for shaft line materials.

Grobe, H. & Alfred Wegener Institute, 2007. Photo from the German research vessel Polarstern port propeller. *Wikimedia Commons*. Available at: https://commons.wikimedia.org/wiki/File:Polarstern_propeller-bb_hg.jpg [Accessed October 28, 2016].

Hoffmann, K., 2001. Applying the Wheatstone bridge circuit. *HBM W1569-1.0 en, HBM, Darmstadt, Germany*, pp.1–28.

Huisman, T.J. et al., 2014. Interaction between warm model ice and a propeller. In *Proceedings of the ASME 2014 33rd International Conference on Ocean, Offshore and Arctic Engineering OMAE2014*. San Francisco, California, USA.

Ikonen, T., Peltokorpi, O. & Karhunen, J., 2014. Inverse ice-induced moment determination on the propeller of an ice-going vessel. *Cold Regions Science and Technology*, 112, pp.1–13.

International Association of Classification Societies, 2011. Requirements Concerning Polar Class. , pp.1–26.

Korean Register, 2015. Guidance for ship for navigation in ice. Available at: http://www.krs.co.kr/KRRules/KRRules2015/KRRulesE.html [Accessed November 10, 2016].

Metallurgica Veneta, 2004. Material specifications for S355J2.

Myklebost, M.R. & Dahler, G., 2013. Agulhas II data analysis of torsional shaft responses from operation in Arctic waters - Technical summary report. *Det Norske Veritas AS*, pp.1–40.

Nieslony, A., 2003. Rainflow counting algorithm. *MathWorks File Exchange*. Available at: https://www.mathworks.com/matlabcentral/fileexchange/3026-rainflow-counting-algorithm [Accessed October 26, 2016].

Polić, D. et al., 2014. Shaft response as a propulsion machinery design load. In *Proceedings of the ASME 2014 33rd International Conference on Ocean, Offshore and Arctic Engineering OMAE2014*. California,.

Rolls-Royce AB, 2010. Whirling calculation. *Report SA1090*, pp.1–15.

Sampson, R., Atlar, M. & Sasaki, N., 2009. Propeller ice interaction - effect of blockage proximity. In *First International Symposium on Marine Propulsors*. Trondheim, Norway.

STX Finland Oy, 2012. Polar supply and research vessel shaft line arrangement.

Tang, B. & Brennan, M.J., 2013. On the influence of the mode-shapes of a marine propulsion shafting system on the prediction of torsional stresses. *Journal of Marine Science and Technology*, 21(2), pp.209–214.

The Alfred Wegener Institut, 2016. Technical data. Available at: http://www.fs-polarstern.de/index.php?lang=EN&aktion=anzeigen&rubrik=015006 [Accessed August 16, 2016].

Transport Safety Agency, 2010. Finnish ice classes equivalent to class notations of recognized classification societies. *Maritime Safety Regulations*.

Transportation Safety Board of Canada, 2010. Statistical summary marine occurences 2010.

Werft Nobiskrug GmbH, 1980. Wellenleitung, Hauptmasse.